

Qualification Tests and Facilities for the ITER Superconductors

P. Bruzzone, R. Wesche, B. Stepanov, F. Cau, M. Bagnasco, M. Calvi, R. Herzog, M. Vogel

Ecole Polytechnique Fédérale de Lausanne (EPFL), Centre de Recherches en Physique des Plasmas, Association EURATOM-Confédération Suisse, CH-5232 Villigen, Switzerland

e-mail contact of main author: pierluigi.bruzzone@psi.ch

Abstract. All the ITER superconductors are tested as short length samples in the SULTAN test facility at CRPP. Eighteen TF conductor samples with small layout variations were tested since February 2007 with the aim of verification of the design and qualification of the manufacturers. The sample assembly and the measurement techniques at CRPP are discussed. Starting in 2010, another test facility for ITER conductors, named EDIPO, will be operating at CRPP to share with SULTAN the load of the samples for the acceptance tests during the construction of ITER.

1. Introduction

The conductor test is a major milestone in all projects for superconducting magnets, to cover the gap between the multifilament strand characterization and the actual properties of large cables. The object of the test is dictated by the operating mode of the magnet and may include the dc performance, ac loss, stability, pressure drop, heat removal rate, etc.

The test of large force flow superconductors is a challenge from the technical and cost point of view. The conductor size calls for a large bore facility (either solenoid or split coil) and the requirement of mimicking the operating conditions calls for a supercritical helium source, high magnetic field and (very) high current source. The test must be “fast and cheap”, to give a quick feed back to the project and to afford a large number of test during the design phase (R&D) and the construction phase (Quality Control).

The SULTAN (SUpraLeiterTestANlage) test facility at CRPP-Villigen was planned thirty years ago with the aim to test high current, force flow superconductors for fusion magnets [1]. Initially designed as a graded solenoid with 600 mm bore to host a single layer conductor sample, fed by a 10 kA direct power supply, SULTAN was upgraded into a split solenoid with 100 mm access gap and a superconducting flux pump to feed the straight, short length sample with current up to 45 kA [2]. Further upgrades included a new current source up to 100 kA in 1996 [3] and pulsed field coils for ac loss and transient stability in 2001 [4].

The test of ITER size cable-in-conduit-conductors (CICC) started in SULTAN in 1998-2001 with the Model Coil conductors, followed by a number of sub-size Nb₃Sn and NbTi CICC for R&D investigations. Most results on the CICC behavior comes from SULTAN experiments, including the quench propagation and detection [5], the transient field stability [6], the role of copper segregation [7], the cyclic load degradation [8], the self field instability [9], the role of the jacket material [10] and cable pattern [11] and the joint optimization [12].

2. The ITER TF Conductor

The Nb₃Sn CICC for the TF coils is the most important ITER conductor because of the large amount of superconductor and its cost. It represents the backbone of the ITER magnet system. At first glance the present TF conductor looks identical to the initial version of 1992, but several changes happened since then. At the begin of the ITER EDA, the TF conductor had an

Incoloy jacket (as in the CSMC), with an excellent match to the coefficient of thermal expansion of the Nb₃Sn. The design temperature margin was 2 K, with current sharing temperature of 8 K at the design field of 13 T [13].

Some of the design changes since 1992 have a “beneficial” impact on the TF conductor: the field is reduced from 13 T to 11.15 T and the Nb₃Sn strand critical current performance improved in the mean time by over 30%. On the other hand, the jacket material is now stainless steel, with a large mismatch of coefficient of thermal expansion compared to Nb₃Sn, and substantial, irreversible degradation was observed in the performance of the Model Coil Nb₃Sn CICC, not accounted in the initial design. The design temperature margin dropped to 0.7 K, with current sharing temperature of 5.7 K at the design field of 11.15 T [14].

The first conductor samples prepared to the 2004 ITER specification were tested in SULTAN in February 2007. The ITER Organization, IO, called representatives of each Domestic Agency, DA, to build a SULTAN Working Group (SWG) with the aim to homogenize the test procedures, in particular, the sample assembly and instrumentation, the test program and data reduction, the result assessment methods and the conductor deliveries, including the test sequence. A total of nine samples (18 TF conductors with minor layout variations) have been tested till June 2008. The actual qualification tests for the ITER TF conductors start in SULTAN as October 2008 and extend to the end of 2009. In the ITER procurement scheme, the result of the qualification samples is crucial to launch the big industrial orders.

2.1. The Current Sharing Temperature Test

The current sharing temperature, T_{cs} , at the nominal operating current and field is the key test for qualification and acceptance of the ITER conductors. The T_{cs} is defined as the conductor temperature at which an average, longitudinal electric field of $10 \mu\text{V/m}$ is observed at $I = 68 \text{ kA}$, in a background field of 10.78 T, corresponding to an effective field of 11.15 T after accounting of the self-field.

In agreement with the SWG, the T_{cs} test for the ITER TF conductors is specified after 1000 load cycles at the nominal $B \times I$ product and a warm-up cycle to room temperature. At constant background field, 10.78 T, the current is raised to 68 kA and then the operating temperature is increased in small steps by heating the coolant until the voltage takes off (quench). The high field voltage signal divided by the spacing of the voltage taps is plotted vs. the temperature downstream of high field: the E - T curve crosses the $10 \mu\text{V/m}$ criterion at T_{cs} .

The E - T curve in Nb₃Sn CICC is characterized by a broad transition from the superconducting to the normal state, as observed since the early prototypes of coils [15] and confirmed in the test of the ITER Model Coils [16]. The reason for the early voltage development is linked to the filament breakages, as it was proven by tests on electromagnetically loaded strands [17].

From the point of view of conductor testing, the broad transition has a large impact on the accuracy of the T_{cs} . As long as the transition is moderately sharp, the gradient dE/dT at $10 \mu\text{V/m}$ is large and the T_{cs} assessment is substantially insensitive to noise and/or voltage offsets. As the n-index of the transition drops to 5 or less, the accuracy of T_{cs} is largely affected by a voltage offset as small as $1 \mu\text{V}$, i.e. $\approx 2 \mu\text{V/m}$ in SULTAN, (dotted lines in Fig. 1), and the crossing of the $10 \mu\text{V/m}$ criterion moves by -0.13 K.

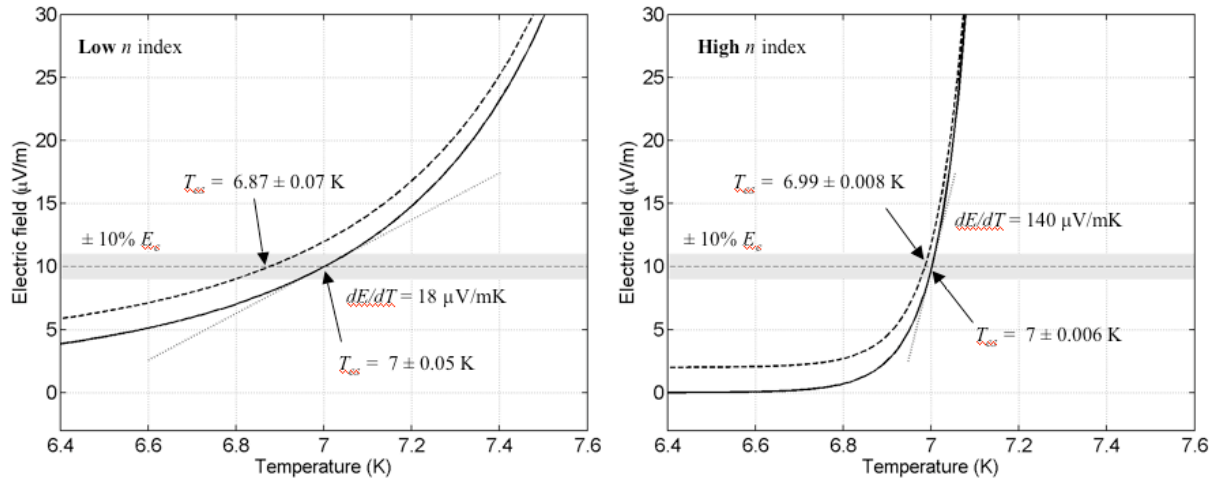


Fig. 1. Examples of broad (left) and moderately sharp (right) transitions. The dotted lines are generated adding an offset of $1 \mu V$ ($\approx 2 \mu V/m$) to the E - T curves

2.2. Sample Preparation, Instrumentation, Data reduction and Post-processing

The assembly of a SULTAN sample starting from two bare conductor sections is carried out at CRPP according to a protocol agreed with the ITER Organization and the SWG. The agreed instrumentation scheme was modified after a number of tests in order to provide a better base for both the electrical and calorimetric assessments of T_{cs} . The final sensor scheme, which will be used for the Qualification Tests, is gathered in Fig. 2. Four temperature sensors are attached upstream and downstream of the high field zone. Two “rings” of voltage taps, spaced by one cable pitch span the high field zone.

During the current ramp from 0 to 68 kA, a potential difference, either positive or negative, with initial slope roughly proportional to the current has been observed in several ITER TF conductor samples. The slope amplitude is in average much larger than observed in previous samples and changes as a function of the background field, operating temperature and history of load cycles. When the amplitude at the end of the current ramp is comparable to the criterion of $10 \mu V/m$, the assessment of T_{cs} from the raw data becomes misleading, see Fig. 3, with a major under- or overestimation of T_{cs} , depending on the polarity of the “voltage slope”.

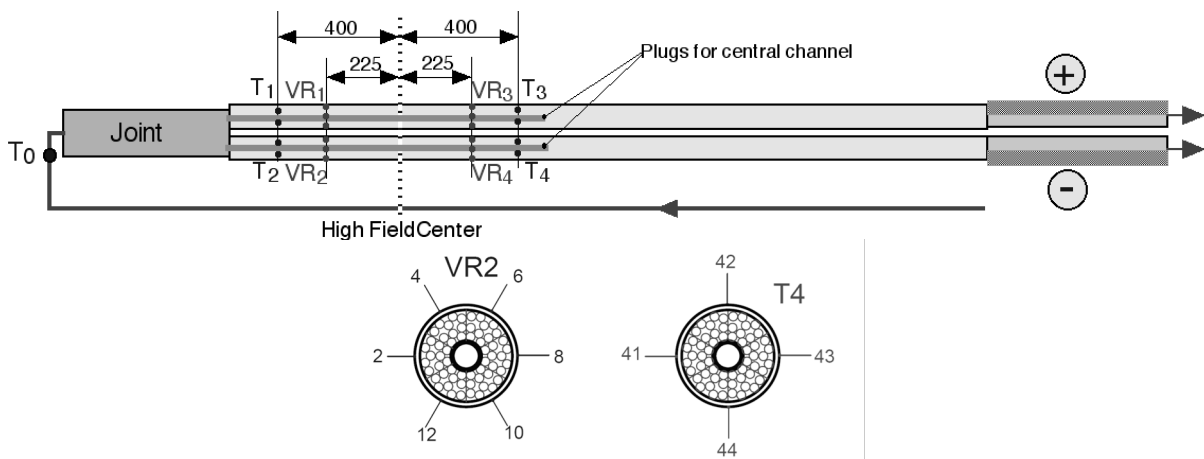


Fig. 2. Instrumentation scheme for the ITER TF qualification samples. The location of the voltage tapping and of the temperature sensor array on the conductor cross section is shown on the bottom

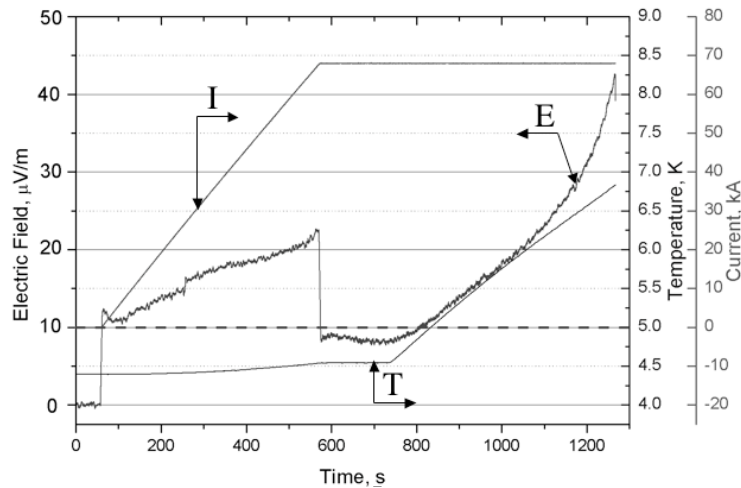


Fig. 3. Example of “voltage slope”, i.e. potential building up during the current ramp in a T_{cs} run

Since the early test campaigns it was observed that the slope/early voltage is not correlated with the expected temperature increase across the high field region and does not generate any measurable power, i.e. it does not represent the “longitudinal” voltage needed for T_{cs} assessment.

In the assumption that the slope is due to transverse potential among the six main sub-cables, arrays of 6 voltage taps (“rings”, see Fig. 2) were applied in an attempt to “average” to zero the transverse voltage. However, the average of the 6 voltage pairs has still a slope. Various locations of “ring” voltage taps have been tried, the best one being at the high field region, spaced by one cable pitch.

The post-processing suggested by the SWG to extract the longitudinal voltage is to average the six signals of the high field ring of voltage taps, assess the initial slope vs. current of the averaged signal, extrapolate to 68 kA and subtract from the raw data. The added value of this procedure is shown in Fig. 4, where the six individual voltage pairs, with result dispersion up to 0.45 K, and the average are compared after the post-processing.

According to one proposed interpretation [18, 19], the slope vs. current originates from the mismatch of contact resistance at the two conductor terminals and is an artifact of the sample

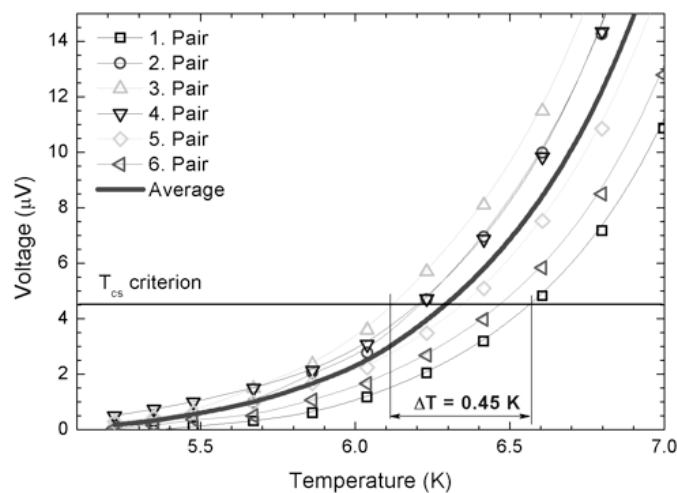


Fig. 4. The T_{cs} from individually post-processed voltage compared to the averaged signal

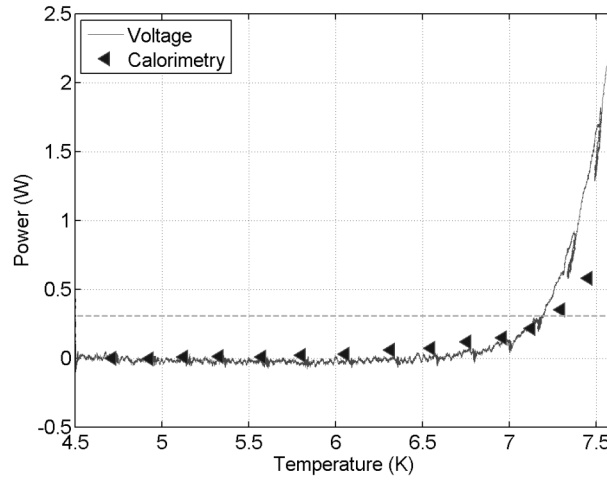


Fig. 5. Comparison of current sharing power by calorimetric and electrical measurements

joints. Such hypothesis calls for a highly non-homogenous resistance distribution at the joint and for very high inter-strand resistance inside the termination. However, the results of resistance distribution and inter-strand resistance in termination [20, 21] do not support the hypothesis and the slopes are much larger than in NbTi CICC, where a similar effect is expected with similar joints. According to another interpretation, the slope is the result of local current re-distribution driven by filament damage. In this case, the slopes are expected to increase with field, temperature and load cycles. This hypothesis implies that almost all strands are affected by filament damage since the cool down, progressing with load cycling.

2.3. Calorimetric Approach for T_{cs} Test

A substantial improvement of the reliability of the temperature measurements was achieved at CRPP in 2007 [22] and made possible an alternative method for the assessment of T_{cs} , based on the calorimetric evaluation of the Joule power, W_{cs} , generated during the current sharing regime. The governing relation for the W_{cs} in steady state is

$$W_{CS} = \dot{m} \left[h(p, T)_D - h(p, T)_U \right], \quad (1)$$

where \dot{m} is the He mass flow rate, h is the He enthalpy as a function of the pressure p and temperature T . The subscripts “U” and “D” refer to the upstream and downstream location, respectively. In the nominal conditions for the T_{cs} tests, the power generated by current sharing at the 0.45 m conductor length exposed to high field is 306 mW, which corresponds to a temperature rise of about 30 mK.

The average reading of the four temperature sensors placed upstream and downstream of the high field zone, see Fig. 2, is retained for the assessment. The redundancy is aimed to minimize the impact of temperature gradients across the cable cross section, which can be as high as 50 mK in the worst cases. The average temperature differences in controlled conditions (i.e. $B_{SULTAN} = 10.78$ T and $I = 0$ kA when the power generated in the high field zone is null) are base-lined to zero to cancel the residual, systematic deviations due to the sensor magneto-resistance. The calorimetric method requires steady state conditions, i.e. the conductor temperature must be raised in steps, which last long enough to establish thermal equilibrium at the high field zone. A comparison of electrical and calorimetric assessment of T_{cs} is shown in Fig. 5 for a conductor which was not affected by large “voltage slope”.

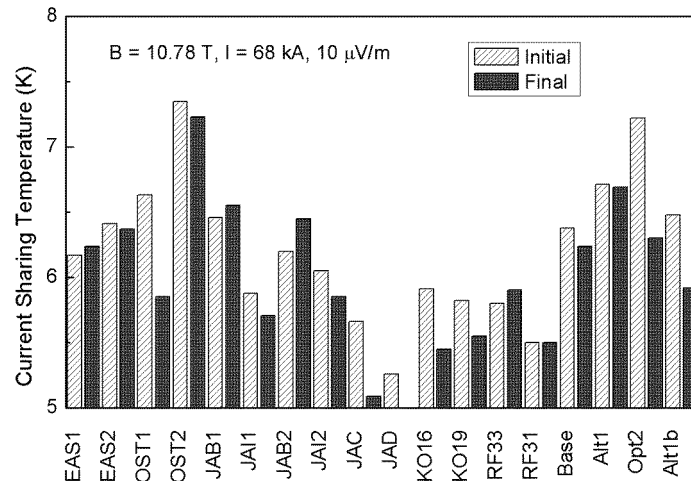


Fig. 6. Current sharing temperature of 18 ITER TF conductors at the first and last run of the test [22]

2.4. Test Results and Discussion

The absolute T_{cs} performance of the 18 conductors at the beginning and end of the test campaign is gathered in Fig. 6 [23]. Whenever applicable, the results are obtained by both post-processing of voltage taps signals and power calorimetry. The error bar is related to the reliability of the post-processing procedure: in most cases it is ± 0.1 K and higher in case of very broad transition.

The potential performance of Nb₃Sn CICC can be derived from the strand scaling laws retaining a pre-fixed thermal strain, $\varepsilon = -0.65\%$, and no degradation. The potential vs. actual performance at the beginning and end of each test campaign is shown in Fig. 7. The spread in the potential performance, x-axis, is due to the different strand properties (total of seven strand suppliers). The mismatch with the potential performance, i.e. the distance from the diagonal, reflects the different load sensitivity of the strands and/or the mitigating effect of the layout variations on the degradation [23]. The few points in the upper half of the plots (conductors with results better than potential) are evidence that the retained thermal strain to calculate the potential performance is too pessimistic.

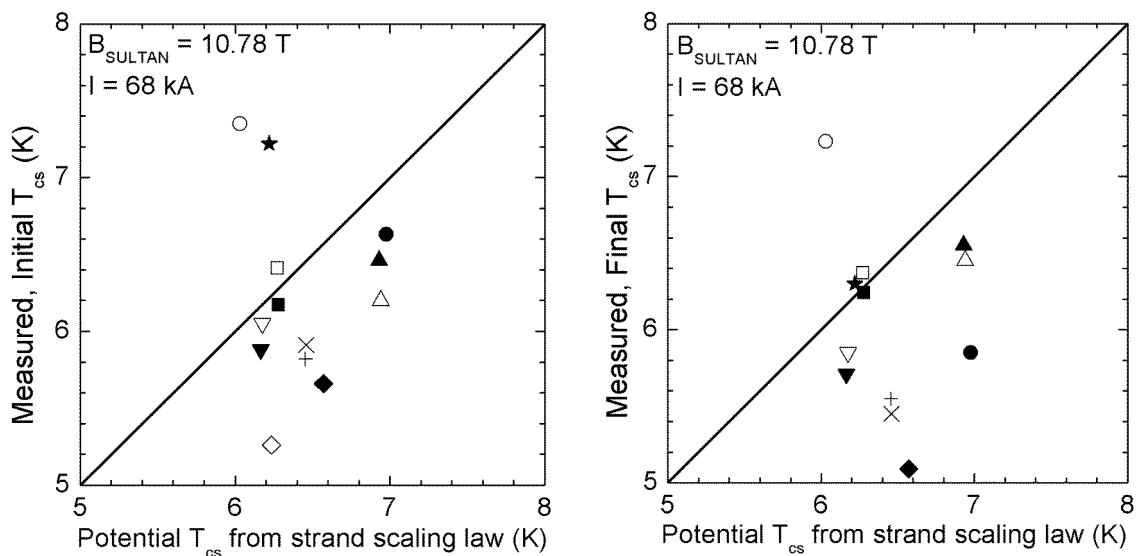


Fig. 7. Potential performance vs. test results for 13 ITER TF conductors

When the superconducting transition is very broad, substantial power is generated at temperature well below the criterion for T_{cs} , see Fig. 1 left. The maximum allowable operating temperature in coils with long conductor lengths exposed to high field must be calculated as a function of the generated power (index loss) and heat removal rate.

The ITER specification has a target of 10 for the index n of the V-I transition. In case of much lower n index, the index loss would become higher and the heat removal rate may need to be increased, e.g. by increasing the mass flow rate and pressure drop over a TF coil.

3. The EDIPO Test Facility

To complement the SULTAN test facility during the ITER construction, when a large number of conductor samples may need to be tested within short term for acceptance, as well as to provide a back-up in case of failure of SULTAN, EFDA has launched in 2004 a second test facility based on a dipole-like winding (tilted head race-track) surrounded by a substantial amount of cold iron to concentrate the flux lines. The project is named EDIPO (European DIPOle). CRPP is the host lab in charge to procure all the components except the superconducting coil, which is supplied by EFDA under industrial contract [24].

Parallel operation of SULTAN and EDIPO at CRPP will be possible if necessary. The two facilities share the same cryo-plant and sample specifications (geometry, sensors, joints, etc.). The peak field in EDIPO is targeted to 12.5 T and the high field length is ≈ 1.1 m, compared to 11 T over ≈ 0.5 m in SULTAN.

The component design, procurement and assembly at CRPP are in progress, the main items being the vacuum vessel, the superconducting current leads, the power supplies, the quench protection system, the superconducting transformer as current source, the control and data acquisition systems. The superconducting winding is scheduled to be delivered to CRPP at the end of 2009 and the commissioning of EDIPO will be in the first half of 2010, see Fig. 8.

4. The Use of the Test Results

The logic of the conductor test, and hence the use of the test results, change substantially according to the project phase. During the R&D and initial design phases, the test has the function of exploring the performance under various operating conditions. The feed back to the design may be either a layout modification or a change of the target for operation. With



Fig. 8. SULTAN and a full scale mock-up of the EDIPO facility (left) at CRPP.

the start of the ITER construction phase and the complex structure of the international procurement, little room is left for a feed back to the design. The aim of the test is now to “qualify” the suppliers and “accept” the delivery. In this context, CRPP, as operator of the test facilities, has the responsibility to provide clear and reliable results to the ITER Organization and Domestic Agencies, who will take decision about acceptance / rejection / non-conformity based on the SULTAN results, with big impact on cost and schedule issues.

The test of the large Nb₃Sn CICC for ITER must face two challenges: on one side the accuracy of the test is poorer due to the broad transition of degraded conductors. On the other hand, the reproducibility of the test results, i.e. of the extent of irreversible degradation, may be limited by definition.

Acknowledgement

This report was prepared as an account of work for the ITER Organization. The Members of the Organization are the People's Republic of China, the European Atomic Energy Community, the Republic of India, Japan, the Republic of Korea, the Russian Federation, and the United States of America. The views and opinions expressed herein do not necessarily reflect those of the Members or any agency thereof. Dissemination of the information in this paper is governed by the applicable terms of the ITER Joint Implementation Agreement.

This work, supported by the European Communities under the contract of Association between EURATOM/Swiss, was carried out within the framework of the European Fusion Development Agreement. The views and opinions expressed herein do not necessarily reflect those of the European Commission.

The technical support of the Paul Scherrer Institute (PSI) is greatly acknowledged.

The authors are indebted to the ITER Organization and the Domestic Agencies for the friendly collaboration during preparation and testing of the ITER TF conductors.

References

- [1] J.D. Elen et al., “The Superconductor Test Facility SULTAN”, IEEE Trans. on Mag. 17, 490-493 (1981).
- [2] E.P. Balsamo et al., “Final Tests of the SULTAN 12 T Facility in the split Coil Configuration”, Fusion Technology 1992, 768-771 (1993).
- [3] G. Pasztor et al., “Design, Fabrication and Testing of a 100 kA superconducting Transformer for the SULTAN Test Facility”, Proc. of MT 15, 839-842, Beijing 1997.
- [4] P. Bruzzone et al., “Upgrade of Operating Range for SULTAN Test Facility”, IEEE Trans. on Appl. Supercon. 12, 520 (2002).
- [5] A. Anghel et al., “The Quench Experiment on Long Length” Final Report CRPP, 1997.
- [6] P. Bruzzone, “Stability under transverse field pulse of the Nb₃Sn ITER cable-in-conduit conductors”, IEEE Trans. on Appl. Supercon. 10, 1062-1065 (2000).
- [7] P. Bruzzone et al., “Test results of SeCRETS, a stability experiment about segregated copper in cable-in-conduit conductors”, IEEE Trans. on Appl. Supercon. 11, 2018-2021 (2001).
- [8] P. Bruzzone et al., “Performance Evolution of Nb₃Sn Cable-in-Conduit Conductors under cyclic Load, IEEE Trans. on Appl. Supercon. 12, 516-519 (2002).

- [9] R. Wesche et al., "Self-Field Effects in NbTi Subsize Cable-in-Conduit Conductors", *Physica C: Superconductivity*, Volume 401, 113-117 (2004).
- [10] N. Martovetsky et al., "Effect of the conduit material on CICC performance under high cycling loads", *IEEE Trans. on Appl. Supercon.* 15, 1367-1370 (2005).
- [11] P. Bruzzone et al., "Transverse Load Degradation in Nb₃Sn Cable-in-conduit Conductors with Different Cable Pattern", *Adv. Cryog. Eng.* 52 B, 558-565 (2006).
- [12] B. Stepanov, et al., "A low Cost Joint for the ITER PF Coils, Design and Test Results", *Fusion Engineering and Design*, 75-79, 259-263 (2005).
- [13] N. Mitchell, "Conductor design for the ITER toroidal and poloidal magnet system", *IEEE Trans. on Mag.* 30, 1602-1606 (1994)
- [14] "ITER Final Design Report", IAEA Vienna and ITER IT Design Description Document 1.1 Update, January 2004.
- [15] P. Rezza, "Mechanical and electrical performance of superconducting cables subject to cyclic stress", Master of Science at MIT, September 1985.
- [16] N. Mitchell, „Summary, Assessment and Implications of the ITER Model Coil Test Results“, *Fusion Engineering Design* 66-68, 971-993 (2003).
- [17] P. Bruzzone et al., "The voltage-current characteristic (n value) of the cable-in-conduit conductors for fusion", *IEEE Trans. on Appl. Supercon.* 13, 1452-1455 (2003).
- [18] N. Martovetsky, "Testing large CICC in short sample configuration and predicting their performance in large magnets", *IEEE Trans. on Appl. Supercon.* 18, 1072-1075 (2008).
- [19] E. P. A. van Lanen, and A. Nijhuis, "Impact of Cabling Pattern, Magnet Field Profile and Joint Properties on Short Sample Qualification Tests of ITER Conductors", to appear in *IEEE Appl. Supercond.* 19
- [20] P. Bruzzone et al., "Test results of contact resistance distribution in NbTi and Nb₃Sn ITER conductor termination", *IEEE Trans. on Appl. Supercon.* 17, 1378-1381, (2007).
- [21] F. Cau et al., "Inter-strand resistance in the termination of ITER conductors", *IEEE Trans. on Appl. Supercon.* 18, 1101-1104 (2008).
- [22] P. Bruzzone et al., "Methods, accuracy and reliability of ITER conductor tests in SULTAN", to appear in *IEEE Appl. Supercon.* 19.
- [23] P. Bruzzone et al., "Qualification Tests for ITER TF Conductors in SULTAN", to appear in *Fusion Engineering and Design*.
- [24] A. Portone et al., "Status of the EDIPO project", to appear in *IEEE Appl. Supercon.* 19.